Supplemental Information

(6 figures and 1 table)

Erythropoietin Synthesis in Renal Myofibroblasts Is Restored by Activation of Hypoxia Signaling

Tomokazu Souma, Masahiro Nezu, Daisuke Nakano, Shun Yamazaki, Ikuo Hirano, Hiroki Sekine, Takashi Dan, Kotaro Takeda, Guo-Hua Fong, Akira Nishiyama, Sadayoshi Ito, Toshio Miyata, Masayuki Yamamoto and Norio Suzuki

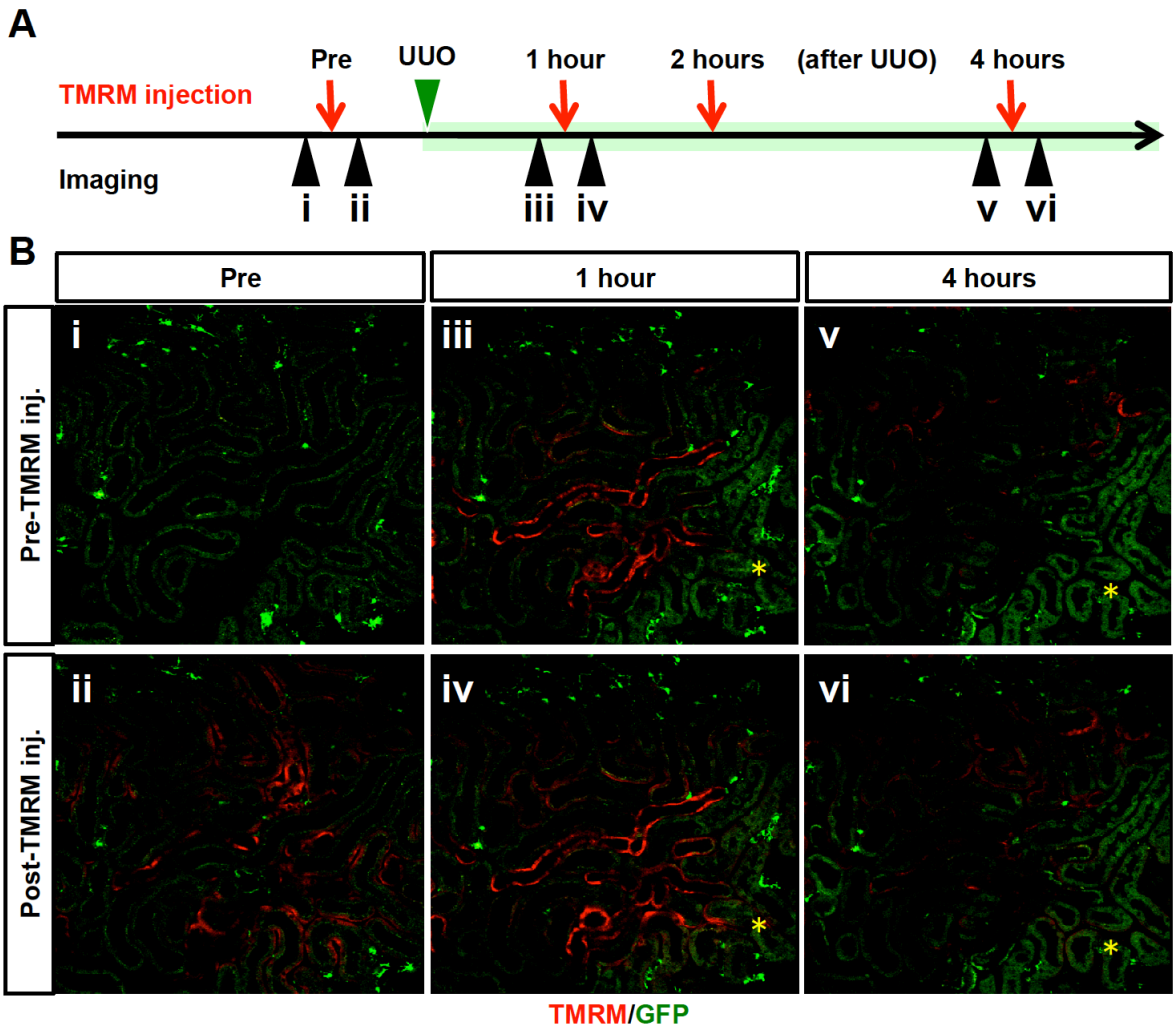

Supplemental Figure 1. Decrease in mitochondrial membrane potential upon injury in ISAM kidneys. (**A**) Schematic protocol for detecting mitochondrial membrane potential in ISAM kidneys by two-photon microscopic imaging at indicated time points (i-vi) before and after UUO treatment. To detect mitochondrial membrane potential, TMRM dye was intravenously injected into ISAM at the indicated time points. (**B**) Activity of the *Epo*-gene transcription (GFP, bright green spots) and mitochondrial membrane potential (TMRM, red) in ISAM kidneys at time points indicated in **A** (i-vi) are shown. Asterisks indicate green auto-fluorescence in tubules. Note that red fluorescence of TMRM was diminished within 4 hours after UUO treatment even with the additional injection of TMRM (vi). GFP signals of ON-REPs are mainly distributed in oxygen-poor areas negative for TMRM signals.

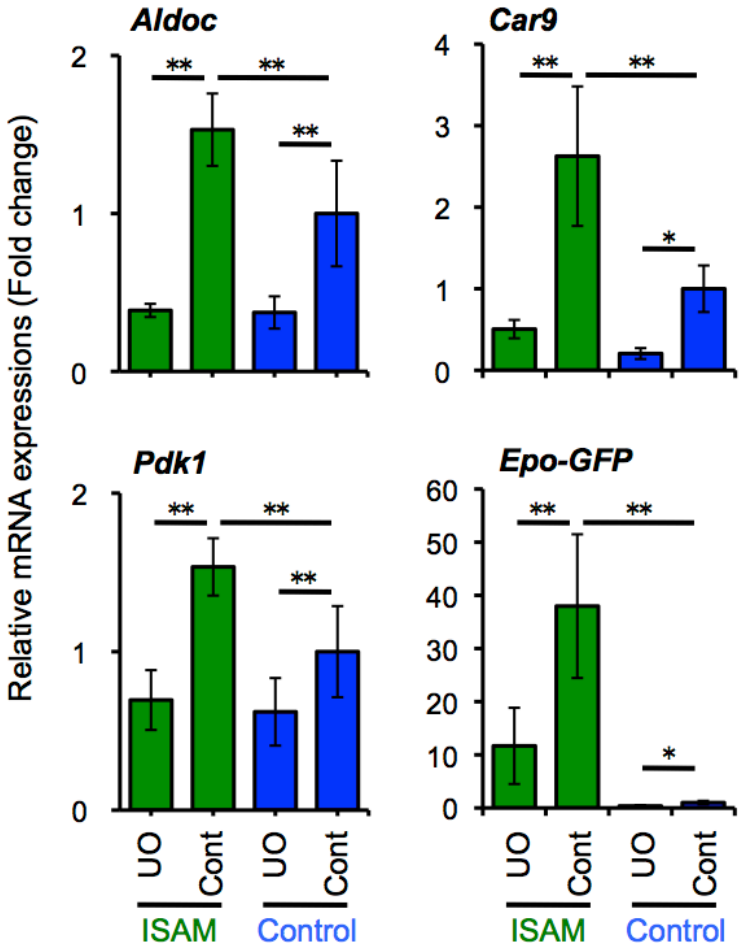

Supplemental Figure 2. Expression of hypoxia-inducible genes in kidneys upon injury. For validation of Figure 3B, RT-qPCR analyses of the indicated genes in the ureteral obstructed (UO) and contralateral (Cont) kidneys of ISAM ($Epo^{GFP/GFP}::Tg^{Epo3'}$ genotype) or the control littermate mice ($Epo^{GFP/wt}::Tg^{Epo3'}$ genotype) were conducted at 2 days after UUO treatment. Data from the contralateral kidneys of control mice were set as 1 (mean±s.d.). *P<0.05, **P<0.01 (n=4) by one-way ANOVA with Tukey-Kramer test for multiple comparisons.

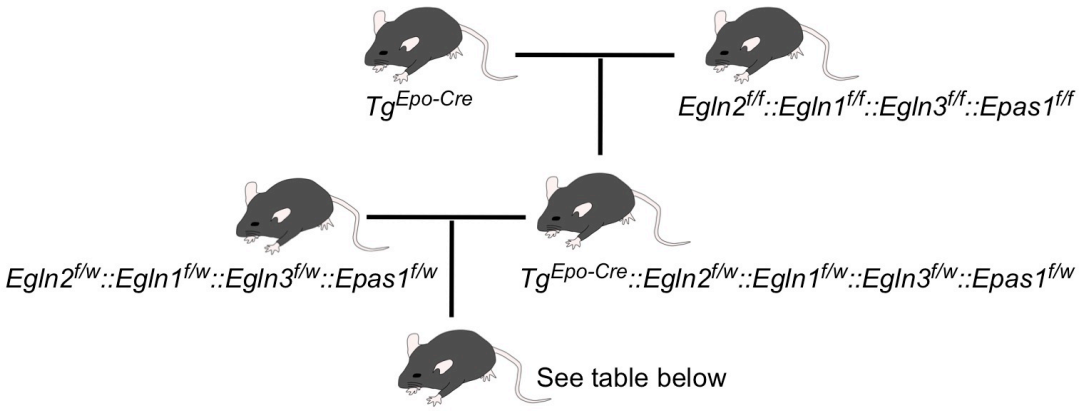

Gene	Protein
Egln1	PHD2
Egln2	PHD1
Egln3	PHD3
Epas1	HIF2α

Nomenclature	Genotype
Control (Cre-)	Mice without $Tg^{Epo\text{-}Cre}$
Control (Cre+)	Mice with $Tg^{Epo\text{-}Cre}$ and each heterozygous allele
P1-EKO	$Tg^{Epo\text{-}Cre}::Egln2^{f/f}::Egln1^{f/w}::Egln3^{f/w}::Epas1^{w/w\ or\ f/w}$
P2-EKO	$Tg^{Epo\text{-}Cre}::Egln2^{f/w}::Egln1^{f/f}::Egln3^{f/w}::Epas1^{w/w\ or\ f/w}$
P3-EKO	$Tg^{Epo\text{-}Cre}::Egln2^{f/w}::Egln1^{f/w}::Egln3^{f/f}::Epas1^{w/w\ or\ f/w}$
P12-EKO	$Tg^{Epo\text{-}Cre}::Egln2^{f/f}::Egln1^{f/f}::Egln3^{f/w}::Epas1^{w/w\ or\ f/w}$
P13-EKO	$Tg^{Epo\text{-}Cre}::Egln2^{f/f}::Egln1^{f/w}::Egln3^{f/f}::Epas1^{w/w\ or\ f/w}$
P23-EKO	$Tg^{Epo\text{-}Cre}::Egln2^{f/w}::Egln1^{f/f}::Egln3^{f/f}::Epas1^{w/w\ or\ f/w}$
P123-EKO	$Tg^{Epo\text{-}Cre}::Egln2^{f/f}::Egln1^{f/f}::Egln3^{f/f}::Epas1^{w/w\ or\ f/w}$
P123H2-EKO	$Tg^{Epo\text{-}Cre}::Egln2^{f/f}::Egln1^{f/f}::Egln3^{f/f}::Epas1^{f/f}$
H2-EKO	$Tg^{Epo\text{-}Cre}::Epas1^{f/f}$

Supplemental Figure 3. Breeding strategy for Epo-producing cell-specific targeting of genes for PHDs and HIF2α.

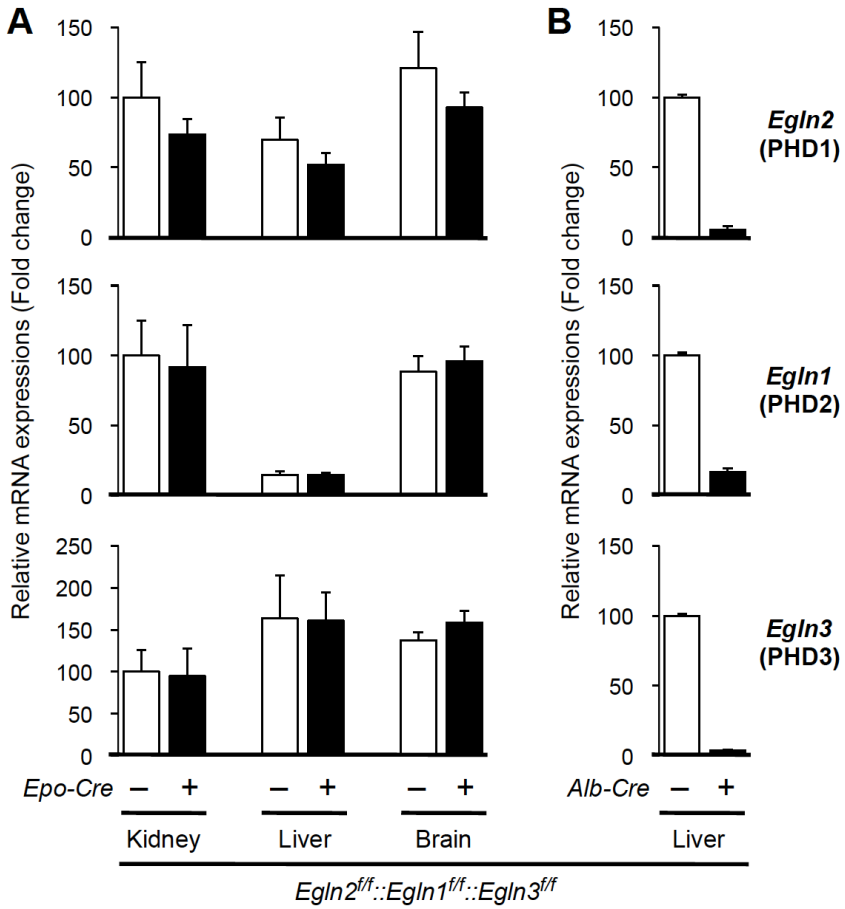

Supplemental Figure 4. Expression of genes for PHDs in kidneys, livers, and brains. (**A**) Gene-targeting efficiency by the *Epo-Cre* transgene. RT-qPCR analyses of genes for PHDs were conducted using P123-EKO (*Epo-Cre*$^{+}$) and the control (*Epo-Cre*$^{-}$) littermate mice. (**B**) Expression levels of genes for PHDs in livers by the *Alb-Cre* transgene. Data from the kidneys (A) or livers (B) of control mice were set as 100 (mean±s.d., n=4). The data indicate that the recombination efficiency of the *Epo-Cre* transgene is very low in whole organ samples, whereas the recombinant efficacy of the *Alb-Cre* transgene, which expresses Cre recombinase exclusively in hepatocytes, is very high.[1] Theses findings are consistent with our previous reports showing that *Epo-Cre*–mediated recombination is induced in a small fraction of total REPs under physiological conditions,[2,3] and that the population of total REPs is less than 5% of the cells in a whole kidney.[3] Therefore, significant changes in levels of mRNAs for PHDs in individual *Epo-Cre*-expressing cells were not observed in whole kidney samples from P123-EKO mice. Polycythemia may be caused by continuous Epo production in a small number of PHD-deficient REPs even though the induction is undetectable in whole kidney samples.

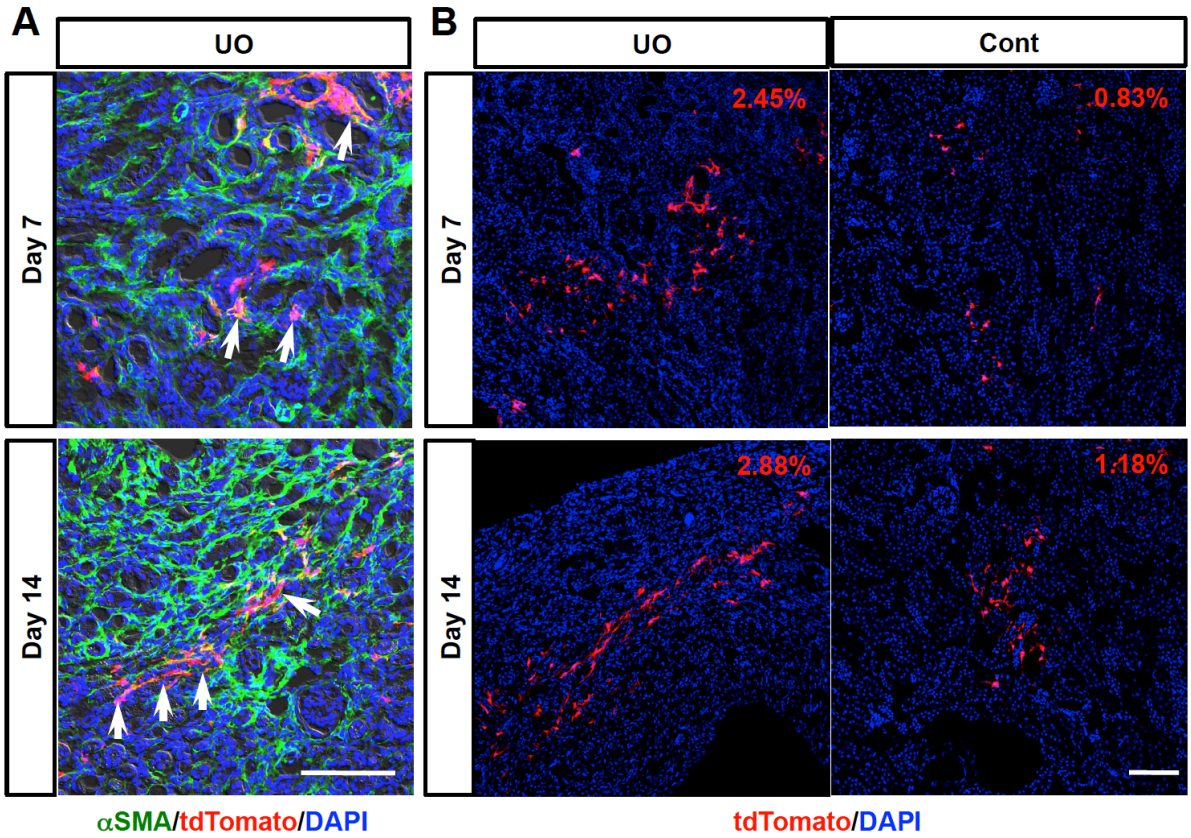

Supplemental Figure 5. Enrichment of MF-REPs in injured kidneys by long-term UUO treatment. (**A**) REPs were tagged and traced with tdTomato expression (red) in kidneys of *R26T::Tg*$^{Epo\text{-}Cre}$ mice.[2] Cryo-sections of kidneys subjected to ureteral obstruction (UO) for 7 and 14 days were stained with αSMA antibodies (green), followed by counterstaining with DAPI (blue). Note that *Epo-Cre*-tagged cells (positive for tdTomato expression) were also positive for αSMA (arrow). (**B**) Enrichment of *Epo-Cre*-tagged cells (red, MF-REPs) in kidneys of *R26T::Tg*$^{Epo\text{-}Cre}$ mice by UO-injury for 7 and 14 days. The percentages of *Epo-Cre*-tagged cells in a cryo-section were calculated relative to DAPI-positive total cells. Scale bars: 100 μm.

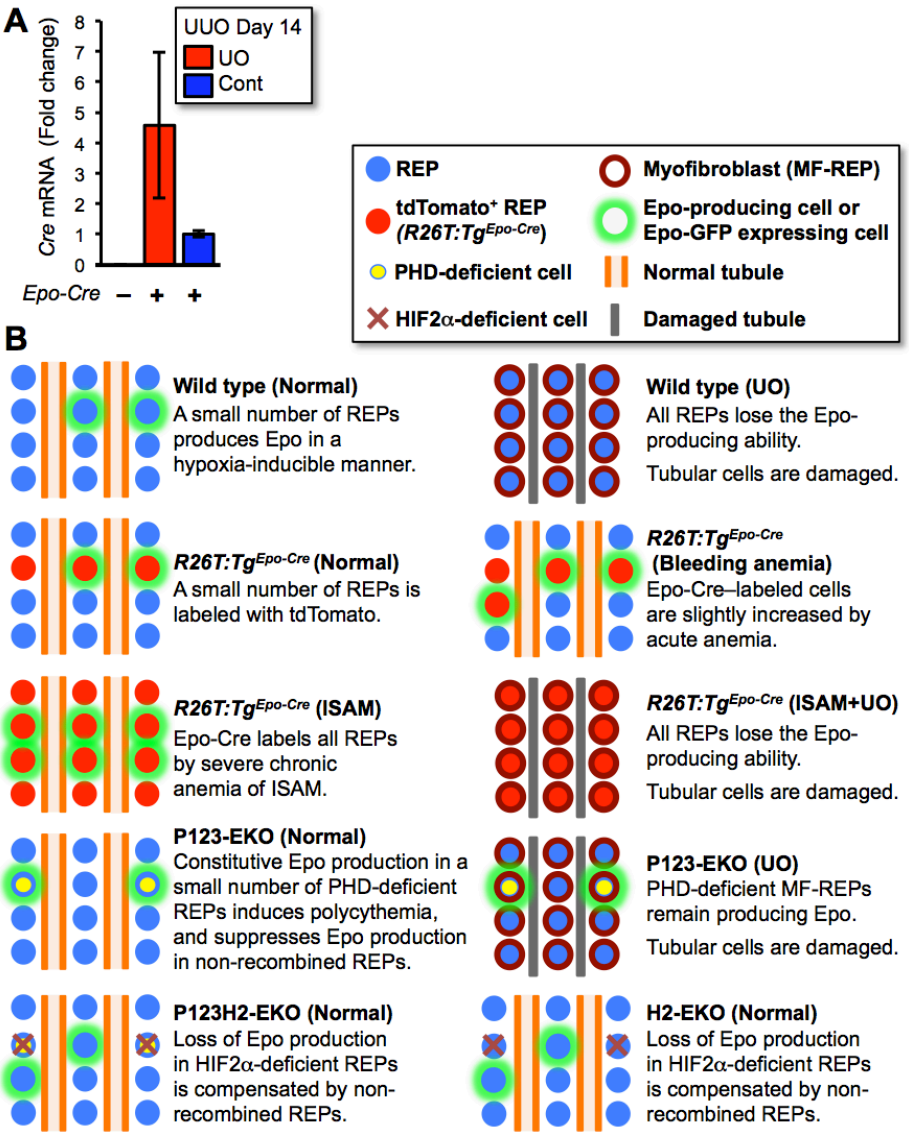

Supplemental Figure 6. The dynamics of Epo-Cre–mediated recombination. (**A**) Expression of the *Epo-Cre* transgene in kidneys from P123-EKO (Cre^{+}) and littermate control (Cre^{-}) mice at 14 days after UUO treatment. Data from the Cont kidneys were set as 1 (mean±s.d., n=3). Similar to the endogenous *Epo*-gene expression, the *Epo-Cre* transgene expression, which is directed by the *Epo*-gene regulatory elements in the BAC-based transgene, is higher in UO-kidneys than the Cont kidneys in P123-EKO mice. (**B**) A schema of Epo-Cre–mediated recombination in normal, anemic, and injured kidneys. Epo-Cre is active only in a small subset of total REPs in *R26T:Tg*$^{Epo\text{-}Cre}$ mice. The activity is slightly enhanced by acute anemia, and almost all REPs are labeled in chronic severe anemia of ISAM.[2,3] The *Epo*-gene expression from P123-EKO kidneys is not higher than that of the control mouse kidneys (see Figure 4E), probably due to suppression of the *Epo*-gene expression in non-recombined REPs by polycythemia of P123-EKO mice. PHD-deficient REPs retain the Epo-producing ability after myofibroblastic transformation.

Supplemental Table 1. Oligo-nucleotide sequences used in this study.

For real-time PCR with SYBR Green

Gene	Sense primer	Antisense primer
Epo-GFP	GGTGGATCCTAAAGCAGCAG	GAAGACTTGCAGCGTGGAC
Acta2	CCCACCCAGAGTGGAGAA	ACATAGCTGGAGCAGCGTCT
Col1a1	AGACATGTTCAGCTTTGTGGAC	GCAGCTGACTTCAGGGATG
Col3a1	TCCCCTGGAATCTGTGAATC	TGAGTCGAATTGGGGAGAAT
Il6	CTGCAAGAGACTTCCATCCAG	AGTGGTATAGACAGGTCTGTTGG
Tnfa	ATGAGAAGTTCCCAAATGGCC	CCTCCACTTGGTGGTTTGCTA
Tgfb1	TGGAGCAACATGTGGAACTC	CAGCAGCCGGTTACCAAG
Itgam	ATGGACGCTGATGGCAATACC	TCCCCATTCACGTCTCCCA
Ptprc	GATTGCTGATGAGGGCAGAC	CTGAATACCCGTGGAATGCT
Emr1	CCTGGACGAATCCTGTGAAG	GGTGGGACCACAGAGAGTTG
Pdk1	GTTGAAACGTCCCGTGCT	GCGTGATATGGGCAATCC
Vegfa	CAGGCTGCTGTAACGATGAA	CTATGTGCTGGCTTTGGTGA
Car9	GCGGATCCACCCGATGGGGA	TGACTGTGGCCACCCCCTTT
Ldha	CGCCCCCCCATCGT	GTTGCCATCTTGGACTTTGAATC
Aldoc	CGTAGGCATCAAGGTTGACA	GAGCACAGCGTTCCAAGAG
Egln1	TAAACGGCCGAACGAAAGC	GGGTTATCAACGTGACGGACA
Egln2	ATGGCTCACGTGGACGCAGTAA	CATTGCCTGGATAACACGCCAC
Egln3	CTATGTCAAGGAGCGGTCCAA	GTCCACATGGCGAACATAACC
Epo-Cre	ACGTTCACCGGCATCAACGT	CTGCATTACCGGTCGATGCA

For real-time PCR primers with Taqman probe

Gene	Sense primer	Antisense primer
rRNA	CGGCTACCACATCCAAGGAA	GCTGGAATTACCGCGGCT
	(**FAM-labeled probe**	TGCTGGCACCAGACTTGCCCTC)
Epo	GAGGCAGAAAATGTCACGATG	CTTCCACCTCCATTCTTTTCC
	(**FAM-labeled probe**	TGCAGAAGGTCCCAGACTGAGTGAAAATA)

For mouse genotyping

Gene	Sense primer	Antisense primer
Egln1	CAAATGGAGATGGAAGATGC	TCAACTCGAGCTGGAAACC
Egln2	TGGGCGCTGCATCACCTGTATCT	ACTGGTGAAGCCTGTAGCCTGTC
Egln3	ATGGCCGCTGTATCACCTGTAT	CCACGTTAACTCTAGAGCCACTGA
Epas1	CAGGCAGTATGCCTGGCTAATTCCAGTT	CTTCTTCCATCATCTGGGATCTGGGACT
$Tg^{Epo3'}$	ACAGGAAGGTCTCACATAGCC	TACAGCTAGGAGAGTTGTGTGG
GFP	CTGAAGTTCATCTGCACCACC	GAAGTTGTACTCCAGCTTGTGC
Cre	ACGTTCACCGGCATCAACGT	CTGCATTACCGGTCGATGCA
R26T	CTGTTCCTGTACGGCATGG	GGCATTAAAGCAGCGTATCC

Supplemental References:

1. Postic, C, Shiota, M, Niswender, KD, Jetton, TL, Chen, Y, Moates, JM, Shelton, KD, Lindner, J, Cherrington, AD, Magnuson, MA: Dual roles for glucokinase in glucose homeostasis as determined by liver and pancreatic beta cell-specific gene knock-outs using Cre recombinase. *J Biol Chem,* 274**:** 305-315, 1999.
2. Yamazaki, S, Souma, T, Hirano, I, Pan, X, Minegishi, N, Suzuki, N, Yamamoto, M: A mouse model of adult-onset anaemia due to erythropoietin deficiency. *Nat Commun,* 4**:** 1950, 2013.
3. Souma, T, Yamazaki, S, Moriguchi, T, Suzuki, N, Hirano, I, Pan, X, Minegishi, N, Abe, M, Kiyomoto, H, Ito, S, Yamamoto, M: Plasticity of renal erythropoietin-producing cells governs fibrosis. *J Am Soc Nephrol,* 24**:** 1599-1616, 2013.